b_{1g}* for minority spin. The net result is spin unpairing of b_{2g} and a_{1g} levels. Mulliken population analysis yields the configuration $Fe^{+1.68}$ 3d(6.09) 4s(0.09) 4p(0.18) with 2.53 unpaired 3d electrons. The calculated contact field is H_c = 330 kG.

In principle one can calculate the electric field gradient for comparison with the measured quadrupole splitting ΔE = 2.6 mm/s.[24] In practice we have found so many large and cancelling contributions across the entire valence band (not to mention core polarization!) that at present there is insufficient numerical precision to make a significant test of this parameter. We are making efforts to correct this deficiency.

Conclusions

Ground state energy levels and charge and spin densities have been calculated for H_2TAP, CuTAP, and FeTAP, using the nonempirical Hartree–Fock–Slater model. The energy levels correlate well with photoelectron binding energies, and it is hoped that X-ray and neutron diffraction data will shortly be available to verify the densities. The local density theory is on less firm ground in treating excitations; however, the simple estimates of optical transitions prove to be useful in validating semiempirical model interpretations. With regard to magnetic and electric hyperfine fields, we find that the simplest MO models used in fitting spin resonance and Mössbauer data omit important polarization (screening) effects which extend across the valence band. With the present computational approach these effects can be crudely mapped, but further development is needed in order to make quantitative hyperfine parameter predictions.

Acknowledgment. Partial support by the National Science Foundation (Grant No. CHE-7812234) and a grant of computer time from the National Resource for Computation in Chemistry is acknowledged. One of us (Z.B.-Y) gratefully acknowledges support through a Chaim Weizmann Fellowship. D.E.E. acknowledges support by the NSF-MRL program through the Materials Research Center of Northwestern University (Grant No. DMR79-23573). We wish to thank Mark Ratner and Joseph Berkowitz for suggestions and encouragement.

Static and Dynamic Stereochemistry of Hexaethylbenzene and of Its Tricarbonylchromium, Tricarbonylmolybdenum, and Dicarbonyl(triphenylphosphine)chromium Complexes

Daniel J. Iverson,[1a] Goeffrey Hunter,[1a,b] John F. Blount,[1c] James R. Damewood, Jr.,[1a] and Kurt Mislow*[1a]

Contribution from the Department of Chemistry, Princeton University, Princeton, New Jersey 08544, and the Chemical Research Department, Hoffmann-La Roche, Inc., Nutley, New Jersey 07110. *Received February 17, 1981*

Abstract: The crystal and molecular structures of hexaethylbenzene (**1**), tricarbonyl(hexaethylbenzene)chromium(0) (**2**), tricarbonyl(hexaethylbenzene)molybdenum(0) (**3**), and dicarbonyl(hexaethylbenzene)(triphenylphosphine)chromium(0) (**4**) have been determined. Crystallographic data for **1**–**4** are collected in Table VI. The methyl groups in **1**–**3** project alternately above and below the least-squares plane of the benzene ring. In **2** and **3**, three of the ethyl groups are eclipsed by the carbonyl groups; the corresponding methyl groups project toward the uncomplexed side of the ring. The barrier to site exchange (ΔG^*) of the ethyl groups in **2** and **3** is ca. 11.5 kcal mol^{-1}, as determined by dynamic NMR spectroscopy. This value is to be compared with the ethyl rotation barrier of 11.8 kcal mol^{-1} estimated for **1** by empirical force field calculations. According to these calculations, the ground-state structure of **1** (D_{3d}) is substantially the same as the conformation in the crystal, and the ethyl group rotations are not correlated (concerted). The structure of **4** differs markedly from those of **1**–**3**, in that all six methyl groups now project toward the uncomplexed side of the ring, and the molecule assumes a staggered rather than an eclipsed conformation (see Figure 6). Several features of the X-ray structure indicate that this conformational change may be ascribed to steric effects of the triphenylphosphine group.

This report deals with stereochemical features of systems in which hexaethylbenzene functions as the η^6-arene in tricarbonylchromium and related transition-metal complexes.[2,3] Hexaethylbenzene is a representative of a class of hexaalkylbenzenes or hexaalkylbenzene analogues in which the alkyl groups are observed or predicted to point alternately up and down around the ring perimeter, so as to impart approximate D_{3d} or S_6 symmetry to the molecule. The parent compound in this class, hexamethylbenzene, has D_{3d} symmetry;[4] other examples are hexakis(bromomethyl)benzene,[5] hexacyclopropylbenzene,[6] MacNicol's "hexa-host" compounds,[7] hexakis(trimethylsilylmethyl)benzene,[8] and the as yet unknown hexaneopentylbenzene.[9,10] The center

(1) (a) Princeton University. (b) On leave from the Department of Chemistry, University of Dundee, Scotland. (c) Hoffmann-La Roche, Inc.

(2) For comprehensive reviews and leading references to the chemistry of tricarbonyl(η^6-arene)transition-metal complexes (M = Cr, Mo, W), see: Sneeden, R. P. E. "Organochromium Compounds"; Academic Press: New York, 1975; p 19 ff. Silverthorn, W. E. In Stone, F. G. A.; West, R., Eds. "Advances in Organometallic Chemistry"; Academic Press: New York, 1975; Vol. 13, p 48 ff. For a recent update on the literature, see: Atwood, J. D. *J. Organomet. Chem.* **1980**, *196*, 79.

(3) A portion of this work was reported in a preliminary communication: Hunter, G.; Iverson, D. J.; Mislow, K.; Blount, J. F. *J. Am. Chem. Soc.* **1980**, *102*, 5942.

(4) Iroff, L. D. *J. Comput. Chem.* **1980**, *1*, 76 and references therein.

(5) Marsau, M. P. *Acta Crystallogr.* **1965**, *18*, 851.

(6) Bar, I.; Bernstein, J.; Christensen, A. *Tetrahedron* **1977**, *33*, 3177.

(7) MacNicol, D. D.; Hardy, A. D. U.; Wilson, D. R. *Nature (London)* **1977**, *266*, 611. MacNicol, D. D.; McKendrick, J. J.; Wilson, D. R. *Chem. Soc. Rev.* **1978**, 65. Hardy, A. D. U.; MacNicol, D. D.; Swanson, S.; Wilson, D. R. *Tetrahedron Lett.* **1978**, 3579. Hardy, A. D. U.; MacNicol, D. D.; Wilson, D. R. *J. Chem. Soc., Perkin Trans. 2* **1979**, 1011. Hardy, A. D. U.; MacNicol, D. D.; Swanson, S.; Wilson, D. R. *Ibid.* **1980**, 999. Freer, A.; Gilmore, C. J.; MacNicol, D. D.; Wilson, D. R. *Tetrahedron Lett.* **1980**, *1159*.

(8) Bock, H.; Kaim, W. *Chem. Ber.* **1978**, *111*, 3552.

(9) Tidwell, T. T. *Tetrahedron* **1978**, *34*, 1855.

0002-7863/81/1503-6073$01.25/0

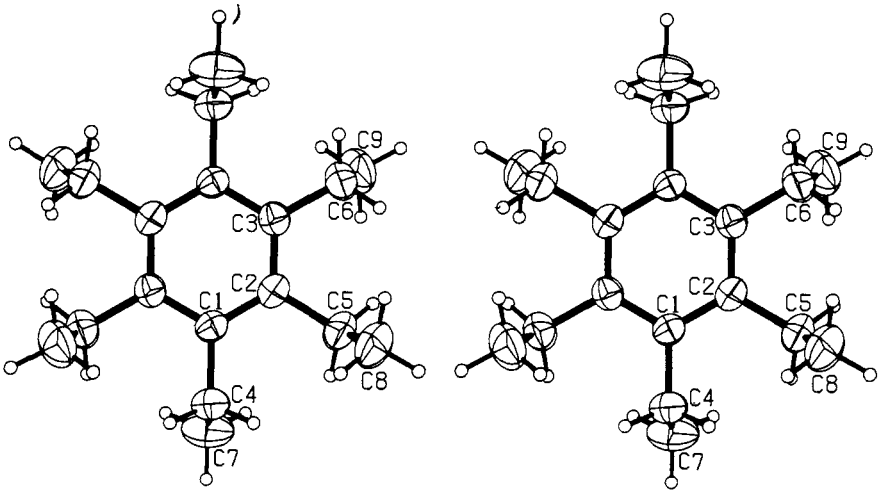

Figure 1. Stereoview of the X-ray structure of hexaethylbenzene (**1**), with the least-squares plane of the benzene ring parallel to the plane of the paper.

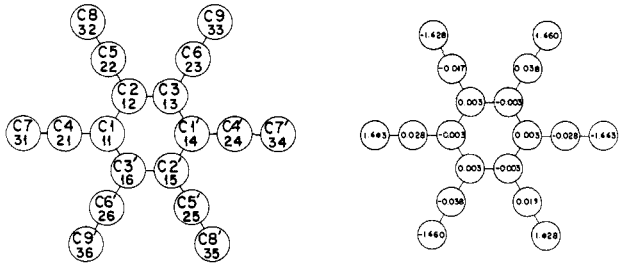

Figure 2. Hexaethylbenzene (**1**). Left: numbering scheme for carbon atoms. For purposes of comparison with the structures shown in Figures 5 and 9, two-digit numerals are also used as indices for C(1) to C(9) and C(1′) to C(9′). Right: deviation (in Å) of carbon atoms from the least-squares plane of the benzene ring.

Table I. Selected Bond Lengths for 1–4[a]

atoms[b]	1	2 (M = Cr)	3 (M = Mo)	4 (M = Cr)
C(11)-C(12)	1.402	1.424	1.427	1.435
C(12)-C(13)	1.403	1.414	1.423	1.421
C(13)-C(14)	1.400	1.424	1.424	1.417
C(14)-C(15)	1.402	1.419	1.425	1.432
C(15)-C(16)	1.403	1.428	1.431	1.404
C(16)-C(11)	1.400	1.417	1.422	1.434
M-C(1)		1.818	1.943	1.803
M-C(2)		1.823	1.948	1.818
M-C(3)		1.828	1.946	
M-C(11)		2.243	2.395	2.199
M-C(12)		2.224	2.362	2.205
M-C(13)		2.240	2.397	2.258
M-C(14)		2.236	2.376	2.299
M-C(15)		2.241	2.402	2.248
M-C(16)		2.223	2.371	2.235
M-P				2.320
C(1)-O(1)		1.162	1.169	1.176
C(2)-O(2)		1.164	1.161	1.162
C(3)-O(3)		1.155	1.165	

[a] In angstrom units. Estimated standard deviations for bond lengths are 0.002–0.003, 0.004–0.006, 0.004–0.006, and 0.001–0.007 Å for 1–4, respectively. [b] Numbering as in Figures 2, 5, and 9. For purposes of comparison with 2–4, the atoms in 1 are renumbered, and two-digit numerals are used as indices for C(1)–C(9) and C(1′)–C(9′) (cf. Figure 2).

of symmetry in D_{3d} and S_6, as well as the C_2 axes in D_{3d}, may be removed upon complexation of the aromatic ring with $M(CO)_3$, TCNE, etc. As a result, the two faces of the benzene ring become nonequivalent and differentiable, and site-exchange phenomena resulting from rotation of the side chains can be monitored by dynamic NMR (DNMR) techniques.

(10) Appropriately substituted hexaphenylbenzenes may also be included in this class. See: Gust, D. *J. Am. Chem. Soc.* **1977**, *99*, 6980. Gust, D.; Patton, A. *Ibid.* **1978**, *100*, 8175.

Table II. Selected Bond Angles for 1–4[a]

atoms[b]	1	2 (M = Cr)	3 (M = Mo)	4 (M = Cr)
C(11)-C(12)-C(13)	120.0	120.7	120.4	119.4
C(12)-C(13)-C(14)	120.1	119.7	119.5	121.2
C(13)-C(14)-C(15)	119.9	120.4	120.9	118.8
C(14)-C(15)-C(16)	120.0	119.1	118.7	120.9
C(15)-C(16)-C(11)	120.1	121.0	121.0	120.1
C(16)-C(11)-C(12)	119.9	119.1	119.2	119.5
C(11)-C(21)-C(31)	112.6	115.7	116.0	115.1
C(12)-C(22)-C(32)	113.1	112.1	112.3	114.6
C(13)-C(23)-C(33)	112.7	116.1	115.6	121.3 (130.2)[c]
C(14)-C(24)-C(34)	112.6	111.9	112.6	113.7
C(15)-C(25)-C(35)	113.1	115.5	115.4	113.4
C(16)-C(26)-C(36)	112.7	111.6	111.8	116.1
C(1)-M-C(2)		89.8	89.4	89.6
C(1)-M-C(3)		88.1	88.4	
C(2)-M-C(3)		88.8	87.4	
M-C(1)-O(1)		177.9	175.9	175.2
M-C(2)-O(2)		178.3	176.8	177.9
M-C(3)-O(3)		179.6	177.7	
C(1)-M-P				89.2
C(2)-M-P				85.4

[a] In degrees. Estimated standard deviations for bond angles are 0.2, 0.2–0.3, 0.2–0.4, and 0.1–0.5° for 1–4, respectively. The standard deviation for C(13)–C(23)–C(33) in 4 is 0.9°. [b] See footnote *b*, Table I. [c] Angle to the maverick methyl C(33)B.

Table III. Selected Dihedral Angles with the Least-Squares Benzene Plane for 1–4[a]

atoms[b,c]	1	2 (M = Cr)	3 (M = Mo)	4 (M = Cr)
C(11)-C(21)-C(31)	89.3	89.2	88.7	89.4
C(12)-C(22)-C(32)	89.3	89.0	90.0	87.7
C(13)-C(23)-C(33)	89.8	88.5	88.5	83.1 (87.5)[d]
C(14)-C(24)-C(34)	89.3	89.6	89.5	87.1
C(15)-C(25)-C(35)	89.3	88.3	88.4	88.8
C(16)-C(26)-C(36)	89.8	90.0	89.2	89.0

[a] In degrees. Estimated standard deviations for dihedral angles are 0.3, 0.3–0.4, 0.3–0.5, and 0.2–0.6° for 1–4, respectively. [b] The atoms which define the second plane. [c] See footnote *b*, Table I. [d] Angle subtended when the maverick methyl, C(33)B, replaces C(33).

Results and Discussion

The Structure of Hexaethylbenzene and of Its Tricarbonylchromium and Tricarbonylmolybdenum Complexes. The molecular structure of hexaethylbenzene (**1**) was determined by X-ray

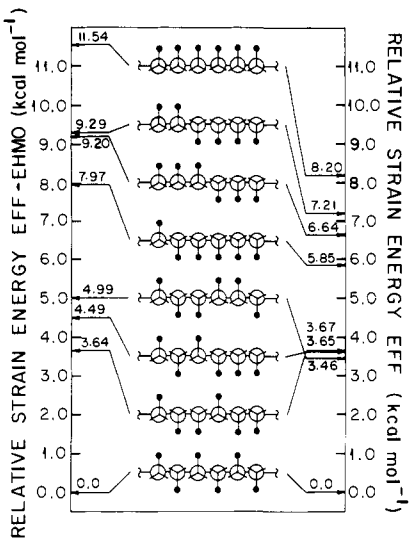

Figure 3. The eight up-down isomers of hexaethylbenzene (**1**). Each schematic projection represents a view around the perimeter of the benzene ring. The heavy dots stand for methyl groups. The scales on the right and left of the diagram indicate relative energies calculated by the EFF (BIGSTRN-2) and EFF–EHMO method, respectively. Reading from the bottom to the top, the isomers, the symmetries of the structures input into BIGSTRN-2, and the symmetries of the resulting optimized geometries are **1a** (D_{3d}, D_{3d}), **1b** (C_{2v}, C_2), **1c** (C_s, C_1), **1d** (C_2, C_2), **1e** (C_s, C_1), **1f** (C_{2h}, C_i), **1g** (C_s, C_1), and **1h** (C_{6v}, C_6).

analysis.[11] The crystals are triclinic, space group $P\bar{1}$, with one molecule per unit cell, in harmony with an earlier report.[12] The molecule is therefore located on a center of symmetry and possesses $\bar{1}$ (C_i) symmetry. A stereoview of the X-ray structure is shown in Figure 1, deviations of the carbon atoms from the least-squares plane of the benzene ring are given in Figure 2, and selected bond lengths, bond angles, and dihedral angles are reported in Tables I–III. The average values of the ring-carbon bond distances (C_{ar}–C_{ar}), the C_{ar}–C_{ar}–C_{ar} bond angles, and the C_{ar}–CH_2–CH_3 bond angles are 1.402 Å, 120.0°, and 112.8°, respectively. The benzene ring is a regular hexagon, very slightly puckered, and there is a small but significant displacement of the methylene carbons away from the least-squares benzene plane (Figure 2) in the direction toward their respective methyl carbons. The average dihedral angle between the C_{ar}–CH_2–CH_3 planes and the least-squares plane of the ring is 89.5°, and the C_{ar}–CH_2–CH_3 planes are therefore essentially perpendicular to the benzene ring. Thus, although there are three independent ring carbon atoms and three independent ethyl groups (the remaining nine carbon atoms of the molecule are generated by the inversion center),[13] i.e., despite the absence of threefold symmetry in the crystal, the molecular symmetry is $\bar{3}m$ (D_{3d}) within the standard deviation of the measurements.

The up–down alternation of ethyl groups in **1** is only one of eight possible arrangements in which the methyl groups are located on one side of the benzene ring plane or the other (Figure 3).

Table IV. Comparison of Experimental and Calculated Structural Parameters of **1a**[a]

atoms[b]	exptl (X-ray)	calcd (EFF)
Bond Lengths		
C(11)–C(12)	1.402	1.402
C(12)–C(13)	1.403	1.402
C(13)–C(14)	1.400	1.402
C(11)–C(21)	1.519	1.532
C(12)–C(22)	1.515	1.532
C(13)–C(23)	1.520	1.532
C(21)–C(31)	1.521	1.540
C(22)–C(32)	1.525	1.540
C(23)–C(33)	1.525	1.540
Bond Angles		
C(11)–C(12)–C(13)	120.0	120.0
C(12)–C(13)–C(14)	120.1	120.0
C(13)–C(14)–C(15)	119.9	120.0
C(11)–C(21)–C(31)	112.6	113.5
C(12)–C(22)–C(32)	113.1	113.5
C(13)–C(23)–C(33)	112.7	113.5
Torsion Angles		
C(16)–C(11)–C(21)–C(31)	89.7	89.6
C(11)–C(12)–C(22)–C(32)	−90.0	−89.6
C(12)–C(13)–C(23)–C(33)	89.0	89.6

[a] Bond lengths in angstroms, angles in degrees. [b] See footnote *b*, Table I.

Since all eight of these forms are in principle interconvertible by rotation of the ethyl groups, there is no reason to exclude, a priori, the possibility that **1** exists in solution as a mixture of several conformational isomers, or even that the D_{3d} structure (**1a**) is a minor component of such a mixture. On this score the NMR spectrum of **1** is uninformative, since C_{ar}, CH_2, and CH_3 each gives rise to only one signal, an observation which is consistent either with the predominance of one relatively stable conformer of the appropriate symmetry (e.g., D_{3d} or C_{6v}), or with a mixture of more or less isoenergetic conformers undergoing rapid interconversion on the NMR time scale. To decide between these alternatives, we resorted to a computational approach: the empirical force field (EFF) method[18] was used to calculate structures and relative energies of the conformers in question. The program employed was BIGSTRN-2.[19] With use of the full relaxation technique (optimization of all structural parameters without symmetry constraints), eight minima were found, corresponding to the eight structural arrangements in Figure 3. Salient features of the structure calculated for **1a** are compared in Table IV with the corresponding parameters found by X-ray analysis; the overall agreement is quite satisfactory.

The tabulation of calculated energies on the right side of Figure 3 shows that **1a** is the ground-state conformer and that the three conformers closest in energy are **1b**, **1c**, and **1d** (3.67, 3.65, and 3.46 kcal mol^{-1} above **1a**, respectively). As a further test of this conclusion, relative energies for the eight structures were computed by the extended Hückel method: such hybrid EFF–EHMO calculations had previously proven useful in the calculation of relative conformational energies.[22] As shown by the tabulation

(11) Crystallographic data and final atomic parameters are listed in the Experimental Section.

(12) Pal, H. K.; Guha, A. C. *Z. Kristallogr., Kristallgeom.*, Kristallphys., *Kristallchem.* **1935**, *A92*, 393.

(13) The molecular C_i symmetry of **1** in the crystal lattice is also discernible by solid-state NMR spectroscopy. Thus all nine crystallographically distinct carbon nuclei have been observed from a single-crystal spectrum of **1**.[14] However, using a crystal *powder*, only five signals were observed (Table V, Experimental Section) in the $^{13}C\{^1H\}$ NMR spectrum.[15]

(14) Pausak, S.; Tegenfeldt, J.; Waugh, J. S. *J. Chem. Phys.* **1974**, *61*, 1338.

(15) Crystallographically distinct but chemically equivalent nuclei are often found to be accidentally isochronous.[14,16,17] The crystal powder NMR pattern may therefore be only a partial reflection of the symmetry imposed by the crystal lattice.

(16) Haeberlen, U. "Advances in Magnetic Resonance Supplement 1"; Academic Press: New York, 1976; p 29.

(17) Hill, H. D. W.; Zens, A. P.; Jacobus, J. *J. Am. Chem. Soc.* **1979**, *101*, 7090.

(18) For recent reviews of the EFF method, see: Dunitz, J. D.; Bürgi, H. B. *MTP Int. Rev. Sci. Org. Chem., Ser. One* **1976**, 81. Ermer, O. *Struct. Bonding (Berlin)* **1976**, *27*, 161. Allinger, N. L. *Adv. Phys. Org. Chem.* **1976**, *13*, *1*. Altona, C.; Faber, D. H. *Fortschr. Chem. Forsch.* **1974**, *45*, 1. See also: Mislow, K.; Dougherty, D. A.; Hounshell, W. D. *Bull. Soc. Chim. Belg.* **1978**, *87*, 555.

(19) Iverson, D. J.; Mislow, K. *QCPE* **1981**, *13*, 410. This program is obtainable from the Quantum Chemistry Program Exchange, Department of Chemistry, Indiana University, Bloomington, Ind. 47401. BIGSTRN-2 uses analytical derivatives of the energy with respect to Cartesian coordinates in steepest descent and/or variable metric[20] minimization procedures. The criterion for the location of an energy extremum is that the root-mean-square of the derivatives falls below a preset value, which is usually 1.0×10^{-4} kcal mol^{-1} Å^{-1}. In addition, BIGSTRN-2 contains all the features of its predecessor, BIGSTRN.[21]

(20) Murtagh, B. A.; Sargent, R. W. H. *Comput. J.* **1970**, *13*, 185.

(21) Andose, J. D. et al. *QCPE* **1978**, *10*, 348.

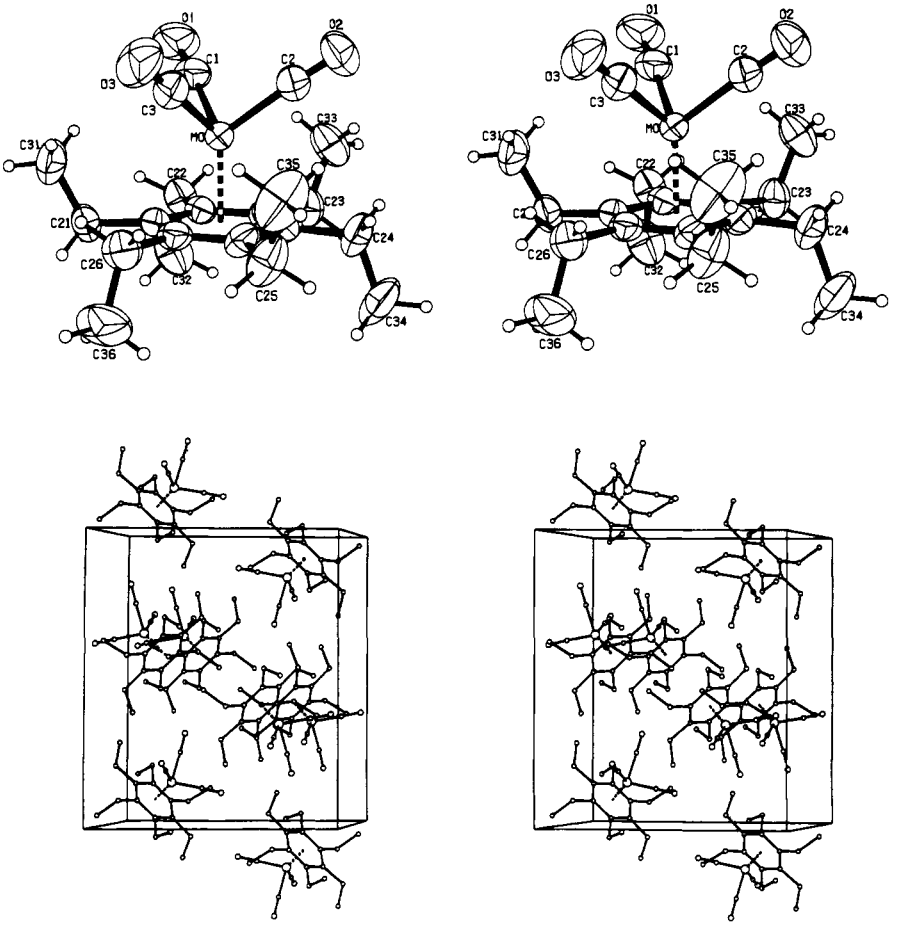

Figure 4. Top: stereoview of the molecular structure of tricarbonyl(hexaethylbenzene)molybdenum(0) (**3**). Bottom: stereoview of the unit cell. The origin is at the lower left rear corner, the *a* (horizontal) and *b* (vertical) axes are parallel to the plane of the paper, and the *c* axis projects toward the observer.

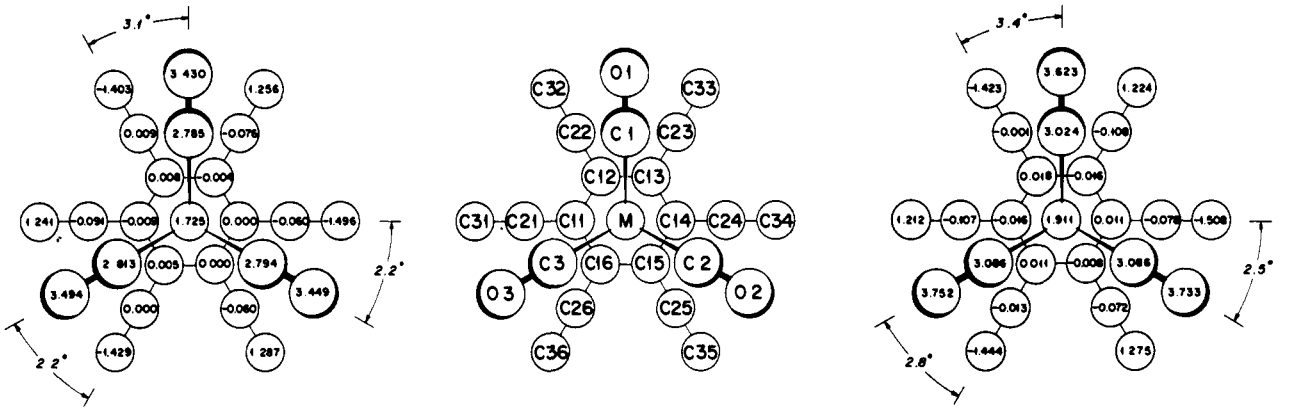

Figure 5. Tricarbonyl(hexaethylbenzene)chromium(0) (**2**) and molybdenum (**3**). Center: numbering scheme for carbon and oxygen atoms (M = Cr or Mo). Left: deviation (in Å) of nonhydrogen atoms in **2** from the least-squares plane of the benzene ring, and selected C_{ar}–X–M–C_{CO} torsion angles (X = centroid of the coordinated arene ring) (a positive value indicates that the terminal methyl carbon is proximal to the metal and a negative value that it is distal). Right: the same for **3**.

of calculated energies on the left side of Figure 3, **1a** remains the ground-state conformer; the conformer closest in energy, **1b**, lies 3.64 kcal mol^{-1} above **1a**. Both methods of calculation therefore predict the same ground-state conformation as found for the X-ray structure, and indicate that solutions of **1** contain more than 99% of this conformer (**1a**) at equilibrium, under normal conditions. Whether any of the higher energy conformers are implicated as intermediates in the degenerate conformational rearrangement (topomerization) of **1a** is a question which will be addressed in the next section.

For reasons adumbrated in the Introduction, we prepared the tricarbonylchromium and tricarbonylmolybdenum complexes of **1** and determined their molecular structures by X-ray analysis.[11] Crystals of tricarbonyl(hexaethylbenzene)chromium(0) (**2**) and tricarbonyl(hexaethylbenzene)molybdenum(0) (**3**) are monoclinic, space group $P2_1/n$, and the two complexes are isomorphous. A stereoview of the X-ray structure of **3** is shown in Figure 4.[23]

(22) Dougherty, D. A.; Mislow, K. *J. Am. Chem. Soc.* **1979**, *101*, 1401. Baxter, S. G.; Fritz, H.; Hellmann, G.; Kitschke, B.; Lindner, H. J.; Mislow, K.; Rüchardt, C.; Weiner, S. *Ibid.* **1979**, *101*, 4493. Dougherty, D. A.; Mislow, K.; Huffman, J. W.; Jacobus, J. *J. Org. Chem.* **1979**, *44*, 1585; Kabalka, G. W.; Jacobus, J. *Ibid.* **1980**, *45*, 1160.

(23) A stereoview of **2** is shown in ref 3.

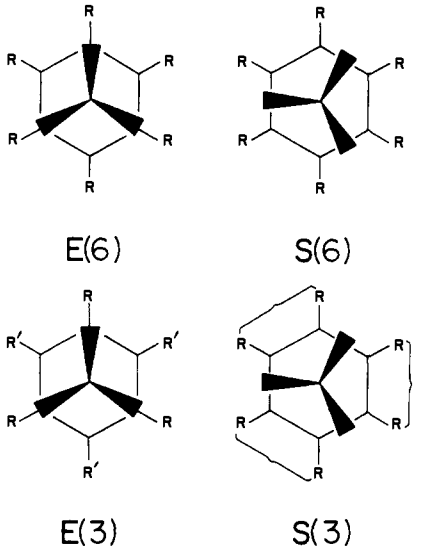

Figure 6. The four structural types of tricarbonyl(η^6-arene)metal complexes with C_{3v} symmetry: **E** = eclipsed, i.e., projection of C–O bonds eclipsing C_{ar}–R or C_{ar}–R′ bonds; **S** = staggered, i.e., projection of C–O bonds bisecting C_{ar}–C_{ar} bonds. The number in parentheses refers to the order of the principal symmetry axis of the arene. Heavy wedges stand for carbonyl bonds projecting toward the observer. Brackets in S(3) indicate symmetric bonding relationships between neighboring R groups, e.g., $(CH_2)_2$ groups.

Deviations of the nonhydrogen atoms from the least-squares plane of the benzene ring are given in Figure 5, and selected bond lengths, bond angles, and dihedral angles are reported in Tables I–III. With the exception of the absolute differences in $M(CO)_3$ atom distances due to the inherent differences in the Cr and Mo bonding radii, both molecules have closely similar structures, with normal[2] bonding parameters (Tables I and II; average M–C_{ar} = 2.235 (M = Cr) and 2.384 (M = Mo)Å). As in **1**, the methyl groups in **2** and **3** project alternately above and below the plane of the ring. The C(1)–C(2)–C(3) and O(1)–O(2)–O(3) planes are parallel (within 1–2°) to the least-squares benzene planes. There are, however, distinctive features which merit further discussion.

The C_{ar}–X–M–C_{CO} (X = centroid of the coordinated arene ring) torsion angles in **2** and **3** are so small (2–3°) that one may properly speak of approximate C_{3v} symmetry. Tricarbonyl(η^6-arene)metal complexes are in principle capable of exhibiting this symmetry only if the arene moiety has three- or sixfold axial symmetry.[24] This restriction leads to precisely four structural types (Figure 6). In the eclipsed structures the ring edges are symmetry equivalent whereas the vertices fall into two symmetry nonequivalent sets of three; conversely, in the staggered structures the vertices are symmetry equivalent whereas the edges fall into two symmetry nonequivalent sets of three. It follows that in the eclipsed structures, there is no requirement for $(C_{ar})_6$ ring planarity and there can be no alternation of C_{ar}–C_{ar} bond lengths; conversely, $(C_{ar})_6$ ring planarity is required of the staggered structures and there is an expectation of C_{ar}–C_{ar} bond alternation. An important distinction exists between C_{3v} complexes of arenes with sixfold and those with threefold axial symmetry:[24] the former are compatible with either a staggered or an eclipsed conformation,[25] whereas in the latter, as illustrated in Figure 6, the substitution pattern determines whether the conformation is staggered or eclipsed; furthermore, two conformational alternatives are always possible for each substitution pattern.[30] To the best of our knowledge, only one X-ray structure has thus far been reported for a tricarbonyl(η^6-arene)metal complex of a D_{3d} or D_{3h} arene (if we discount hexamethylbenzene[25]), that of tricarbonyl(1,3,5-trimethylbenzene)molybdenum(0).[28] This molecule adopts the **E**(3) conformation with R = CH_3 and R′ = H; the preference over the alternative conformation with R = H and R′ = CH_3 must be primarily electronic in origin.[2,31] However, in the case of **2** and **3**, which also adopt E(3) conformations,[32] the preference is unlikely to be electronic in origin, since R = R′ = C_2H_5. We are therefore dealing with a predominantly steric effect: in the noneclipsed R′ groups the methyl groups project toward the complexed (proximal) side of the ring, whereas in the eclipsed R groups they project toward the uncomplexed (distal) side. Evidently, this particular arrangement is the result of nonbonded repulsive interactions between carbonyl and methyl groups.

It is also instructive to compare structural features of the complexed hexaethylbenzene moiety in **2** and **3** with corresponding features in the free arene. There is an overall similarity: in both cases, methyl groups project alternately above and below the plane of the benzene ring, with the C_{ar}–CH_2–CH_3 planes essentially perpendicular to the latter. However, there are also some significant differences that result from the desymmetrization attending complexation. First, the C_{ar}–CH_2–CH_3 bond angles of the eclipsed and noneclipsed ethyl groups differ appreciably: the average value is 111.9° (112.2°) for the eclipsed groups in **2** (**3**), i.e., close to the value of 112.8° in **1**, whereas the corresponding value for the noneclipsed groups is 115.8° (115.7°). Second, those C_{ar}–C_{ar}–C_{ar} angles whose central atoms are eclipsed by the carbonyl groups have an average value of 120.7° (120.8°) in **2** (**3**), whereas the average value for the other angles is 119.3° (119.1°). Third, the terminal carbons of the noneclipsed ethyl groups in **2** and **3** are ca. 0.2 Å closer to the plane of the benzene ring than they are in **1**, whereas the corresponding distances in the eclipsed groups remain essentially unchanged; concomitantly, the methylene carbons on the noneclipsed groups retreat ca. 0.08 Å to the other side of the ring, in contrast to **1**, where the methylene carbons are found about 0.03 Å from the plane of the ring on the same side as their methyl carbons. And fourth, the average dihedral angle between the least-squares plane of the benzene ring and the C_{ar}–CH_2–CH_3 planes is about 1° smaller for the noneclipsed ethyl groups, 88.7° (88.5°) for **2** (**3**), than for the eclipsed ones, 89.5° (89.6°). There is a further difference, though one which is not directly related to the change in symmetry: the average C_{ar}–C_{ar} bond distance in **2** (**3**), 1.421 Å (1.425 Å),[33] is lengthened relative to that in **1** by ca. 0.02 Å.[34]

An interesting comparison may also be drawn between the structures of **1** and **2** and those of the isoelectronic borazine analogues. As in **1**, the methyl groups in hexaethylborazine

(24) Dihedral symmetry is assumed for the free arene. When the symmetry is C_{3h} or C_{6h}, complexation with $M(CO)_3$ leads to a pair of enantiomeric C_3 or C_6 structures.

(25) However, only staggered (S(6)) conformations have thus far been reported. Tricarbonylbenzenechromium(0)[26] is an example, as are tricarbonyl(hexamethylbenzene)chromium(0)[27] and tricarbonyl(hexamethylbenzene)molybdenum(0)[28] if the methyl groups are considered conically symmetric for purposes of classification. Although the arene retains near D_{3d} symmetry in its TCNE complex[29] (and presumably in the tricarbonylmetal complexes as well), the approximation of near D_{6h} symmetry reflects the reasonable assumption that differences in the conformations of the methyl groups will have a negligible effect on the conformation of the $M(CO)_3$ moiety.

(26) Bailey, M. F.; Dahl, L. F. *Inorg. Chem.* **1965**, *4*, 1314. Rees, B.; Coppens, P. *Acta Crystallogr., Sect. B* **1973**, *B29*, 2516.

(27) Bailey, M. F.; Dahl, L. F. *Inorg. Chem.* **1965**, *4*, 1298.

(28) Koshland, D. E.; Myers, S. E.; Chesick, J. P. *Acta Crystallogr., Sect. B* **1977**, *B33*, 2013.

(29) Maverick, E.; Trueblood, K. N.; Bekoe, D. A. *Acta Crystallogr., Sect. B* **1978**, *B34*, 2777.

(30) Only one is shown for E(3) and S(3) in Figure 6. The other conformation is generated by a 60° twist of the $M(CO)_3$ moiety.

(31) Sim, G. A. *Ann. Rev. Phys. Chem.* **1967**, *18*, 57.

(32) The solid-state NMR spectrum of **2** is consistent with the observed threefold symmetry (Table V, Experimental Section).[15] See also: Maricq, M. M.; Waugh, J. S.; Fletcher, J. L.; McGlinchey, M. J. *J. Am. Chem. Soc.* **1978**, *100*, 6902. These authors tentatively conclude that the ring carbons attached to the noneclipsed ethyl groups give rise to the higher field line at 111.0 ppm.

(33) The apparent bond lengths alternation in **2** (Table I) is not significant in terms of standard deviations. Such bond alternation is also disallowed on grounds of symmetry under the C_{3v} approximation (see text).

(34) Substantial bond lengthening effects have also been observed in tricarbonyl(hexamethylbenzene)transition-metal complexes[27,28] and are in one case[28] accompanied by the bond alternation expected of S(6) conformations (see text).

Table V. NMR Properties of Compounds 1-4

compd	nucleus	solvent	temp,[b] °C	resonance freq[a] CH_3	CH_2	C_{ar}	CO	PPh_3
1	$^{13}C\{^1H\}$	CD_2Cl_2		15.5	21.6	137.2		
	$^{13}C\{^1H\}$	neat		15.4, 16.7, 18.0	24.0	137.2		
	^1H	$CDCl_3$		1.18 (t)[c]	2.64 (q)[c]			
2	$^{13}C\{^1H\}$	CD_2Cl_2		17.0	21.6	114.4	235.4	
	$^{13}C\{^1H\}$	CD_2Cl_2	−71	14.2, 20.1	19.4, 22.8	108.8, 117.2	235.4	
	$^{13}C\{^1H\}$	neat		14.6, 21.1, 25.0[d]	23.5,	111.0, 118.5	237.8[d]	
	^1H	$CDCl_3$		1.25 (t)[e]	2.4 (q)[e]			
3	$^{13}C\{^1H\}$	CD_2Cl_2		19.2	22.1	118.5	225.1	
	$^{13}C\{^1H\}$	CD_2Cl_2	−67.5	14.4, 23.4	19.5, 22.8	114.7, 121.6	225.0	
	^1H	$CDCl_3$/ $CFCl_3$		1.24 (t)[f]	2.44 (q)[f]			
4	$^{13}C\{^1H\}$	CD_2Cl_2		16.9	23.4	109.2	243.6[g,h]	127.7, 128.0, 128.8, 133.4, 133.8, 140.7
	$^{13}C\{^1H\}$	CD_2Cl_2	−84	15.9	22.4	108.0	243.5[g,h]	127.0, 127.3, 128.0, 131.0, 132.6
	$^{13}C\{^1H\}$	$CHFCl_2$	−125	16.15	23.37		245.0[h]	
	$^{13}C\{^1H\}$	neat		18.8	25.0	104.5, 104.5, 107.1, 109.1, 111.7, 114.6	242.3,[g,i] 247.6[g,i]	129.4, 133.8, 135.7, 139.1, 144.0, 146.8
	^1H	CD_2Cl_2		1.14 (t)[k]	2.27 (q)[k]			7.4 (m)
	$^{13}P\{^1H\}$	CD_2Cl_2						92 (s)[l,m]

[a] For solution spectra, chemical shifts are in parts per million downfield from internal tetramethylsilane (unless otherwise specified). For $^{13}C\{^1H\}$ spectra in CD_2Cl_2, assignments were made by use of single frequency off-resonance decoupling. [b] Ambient temperatures (30–35 °C) unless specified otherwise. [c] $^3J_{HH}$ = 7.5 Hz. [d] The peak has an additional shoulder. [e] $^3J_{HH}$ = 7.1 Hz. [f] $^3J_{HH}$ = 7.4 Hz. [g] Observed on ^{13}CO-enriched material. [h] $^2J_{PC}$ = 22.3 Hz. [i] $^2J_{PC}$ = 19.5 Hz. [j] $^2J_{PC}$ = 23.4 Hz. [k] $^3J_{HH}$ = 7 Hz. [l] Referenced to external H_3PO_4. [m] In addition to the singlet, the expected doublet and triplet ($^2J_{PC}$ = 22.3 Hz) were also observed in the ^{13}CO-enriched material.

alternately project above and below the ring plane.[35] However, in tricarbonyl(hexaethylborazine)chromium(0), which otherwise closely resembles **2**, the alternation is interrupted by one of the three noneclipsed *N*-ethyl groups, whose methyl is distal instead of proximal (the three *B*-ethyl groups are all eclipsed and their methyls distal).[36] This effect has been ascribed[36] to borazine ring puckering in the complex.

Stereodynamics of Ethyl Group Rotation. The 25.2-MHz $^{13}C\{^1H\}$ NMR spectrum of **2** and **3** in CD_2Cl_2 displays four signals at ambient temperatures, corresponding to the CH_3, CH_2, C_{ar}, and CO carbons (Table V, Experimental Section). At temperatures below 10 °C, the CH_3, CH_2, and C_{ar} signals broaden; below −30 °C decoalescence is complete and each of the three signals has split into two. The coalescence phenomenon reflects a topomerization of the molecule in which the diastereotopic ethyl groups undergo site exchange.[37] Rates of exchange were obtained by line-shape analysis of the C_{ar} line coalescence by using the program DNMR3,[38] and a least-squares fit of the rate data to the Eyring equation (assuming a transmission coefficient of unity) yielded values of $\Delta G^{\ddagger}_{300}$ = 11.5 ± 0.6 and 11.6 ± 0.2 kcal mol^{-1} for **2** and **3**, respectively.

What is the mechanism responsible for this topomerization? A variety of stepwise rearrangements are conceivable, all of which may be represented as subgraphs of the rearrangement graph for **1** (Figure 7), with loops and multiple edges added where necessary. The rotation of the ethyl groups may be completely uncorrelated, i.e., only one ethyl group may move at a time from an up to a down position. An example is **1a** → **1c** → **1e** → **1g** → **1f** → **1c** → **1a**. Alternatively, the motion may be partially correlated, as, for example, in **1a** → **1e** → **1d** (or **1f**) → **1a**, where the motions of two ethyl groups are coupled, or as in **1a** → **1b** (or **1g**) → **1a**, where the motions of three groups are coupled. Completely

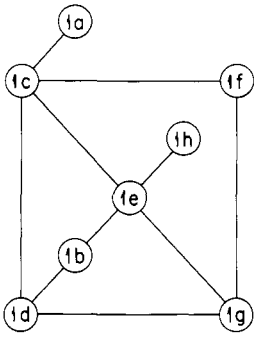

Figure 7. Rearrangement graph for hexaethylbenzene (**1**). The circled symbols represent the eight up–down conformers of **1** shown in Figure 3, and each edge represents a change of one ethyl group from an up to a down position.

correlated rotation, **1a** → **1a**, implies coupled rotation of all six ethyl groups in a concerted process, i.e., by way of a single transition state. In order to decide among these alternatives, ethyl group rotation of **1a** was simulated by EFF calculations, using the incremental group driving technique and the program BIGSTRN-2.[19] The torsion angle ϕ (C(2)–C(1)–C(4)–C(7)) was frozen at decreasing values,[39] while all other internal parameters were minimized with respect to energy. The favored rearrangement pathway was found to be completely uncorrelated, **1a** → **1c** → **1d** → **1b** → **1d** → **1c** → **1a**, with a calculated barrier height of 11.8 kcal mol^{-1} (**1a** → **1c**).[40]

The excellent agreement between calculated and found topomerization barriers may be somewhat fortuitous since the calculation refers to the free arene, whereas the experimental values were determined on the π-complexes. Complexation may

(35) Viswamita, M. A.; Vaidya, S. N. *Z. Kristallogr., Kristallgeom., Kristallphys., Kristallchem.* **1965**, *121*, 472.
(36) Huttner, G.; Krieg, B. *Angew. Chem., Int. Ed. Engl.* **1971**, *10*, 512; *Chem. Ber.* **1972**, *105*, 3437.
(37) A site-exchange process involving arene-metal bond dissociation was ruled out by the observation of separate resonances in a mixture of **1** and the transition-metal complex at ambient temperature.
(38) Kleier, D. A.; Binsch, G. *QCPE* **1970**, *11*, 165.
(39) The torsional angle ϕ was held fixed at a given value (ϕ_0) by imposing a large quadratic potential, E_{fix} = 10000 ($\phi - \phi_0$)^2 kcal mol^{-1}. This technique is a modified version of one originally employed: Wiberg, K. B.; Boyd, R. H. *J. Am. Chem. Soc.* **1972**, *94*, 8426.
(40) According to our calculations, the completely correlated (concerted) rearrangement of all six ethyl groups requires a substantially higher barrier (>30 kcal mol^{-1}).

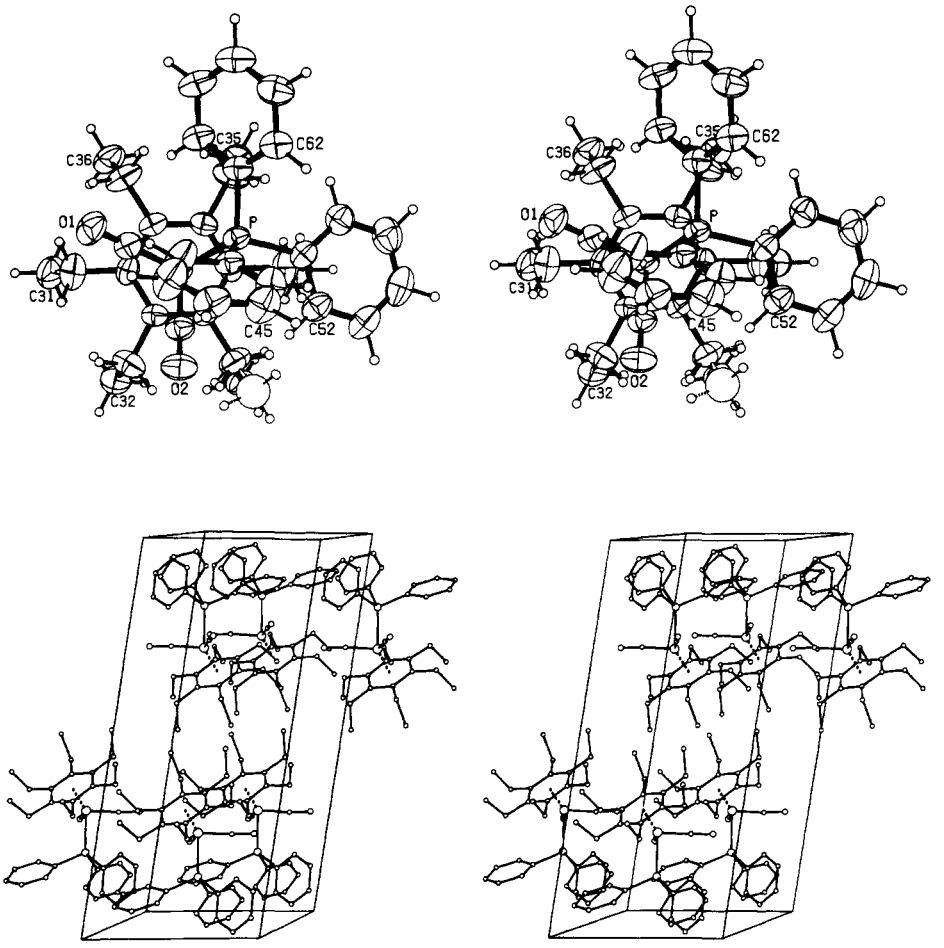

Figure 8. Top: stereoview of the molecular structure of dicarbonyl(hexaethylbenzene)(triphenylphosphine)chromium(0) (**4**). The maverick ethyl group is shown by dashed bonds and an open circle representing the methyl carbon. Bottom: stereoview of the unit cell. The origin is at the lower left rear corner, the *b* (horizontal) and *c* (vertical) axes are parallel to the plane of the paper, and the *a* axis projects toward the observer.

have a far from negligible effect on the barrier,[41] and it is possible that the barrier heights for **1** and **2** (or **3**) differ by as much as ca. 2 kcal mol^{-1}, given the error limits in the EFF estimate.[18] Nevertheless, there is no uncertainty about the major conclusion: ethyl rotations in **1–3** are uncorrelated.

In connection with the study described above, it was also of interest to determine the barrier to rotation about the arene–metal bond axis. A reorientation barrier of 2.7 kcal mol^{-1} was determined for **2** from the slope of a least-squares plot of ln R_1^{DD}[42] vs. T^{-1}. This barrier includes contributions from overall molecular tumbling and internal rotation about the arene–metal bond, but attempts to obtain an independent measure of the overall molecular tumbling proved unsuccessful. We are therefore unable to provide a reliable estimate of the arene–chromium rotation barrier. However, by analogy with other tricarbonyl(η^6-arene)chromium complexes,[44] we believe that the barrier is unlikely to exceed ca. 5 kcal mol^{-1}.[44,45]

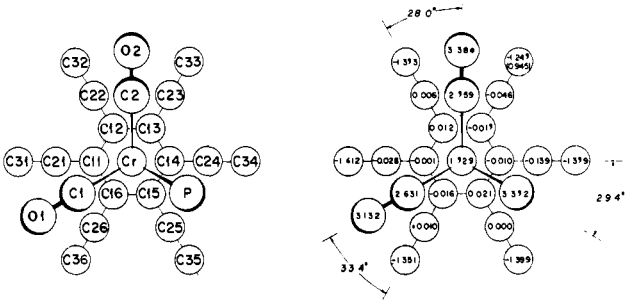

Figure 9. Dicarbonyl(hexaethylbenzene)(triphenylphosphine)chromium-(0) (**4**). Left: numbering scheme for carbon and oxygen atoms. Right: deviation (in Å) of nonhydrogen atoms from the least-squares plane of the benzene ring and selected C_{ar}–X–Cr–C_{CO} (or P) torsion angles. A positive value indicates that the terminal methyl carbon is proximal to the metal and a negative value that it is distal. The parenthesized value refers to C(33)B, the maverick methyl carbon.

Dicarbonyl(hexaethylbenzene)(triphenylphosphine)chromium(0). Ultraviolet irradiation of a heptane solution of **2** in the presence of an excess of triphenylphosphine yielded an orange-yellow precipitate of **4**. The structure of **4** was determined by X-ray

(41) For example, the barrier to rotation ($\Delta G^{\ddagger}$) about the aryl–alkyl single bond in tricarbonyl(2,2,4,4-tetramethyl-3-phenylpentane)chromium(0) is 16.9 kcal mol^{-1}, as compared to 22.2 kcal mol^{-1} for the corresponding barrier in 2-nitro-4-(2′,2′,4′,4′-tetramethyl-3′-pentyl)acetanilide: van Meurs, F.; Baas, J. M. A.; van der Toorn, J. M.; van Bekkum, H. *J. Organomet. Chem.* **1976**, *118*, 305. However, in less crowded systems, such as **1–3**, the barrier difference is expected to be much smaller: Iverson, D. J.; Mislow, K. *Organometallics*, in press.

(42) The C–H dipolar relaxation rate (R_1^{DD}) of the carbonyl carbons was calculated from the total spin-lattice relaxation time and the nuclear Overhauser enhancement (see Experimental Section).[43a]

(43) Wehrli, F. W.; Wirthlin, T. "Interpretation of Carbon-13 NMR Spectra"; Heyden: London, 1978: (a) pp 147–148; (b) pp 140–142.

(44) (a) Albright, T. A.; Hofmann, P.; Hoffmann, R. *J. Am. Chem. Soc.* **1977**, *99*, 7546 and references therein. (b) Delise, P.; Allegra, G.; Mognaschi, E. R.; Chierico, A. *J. Chem. Soc., Faraday Trans. 2* **1975**, *71*, 207.

(45) A substantially higher barrier in transition-metal complexes of benzene derivatives seems to require bulky substituents on the metal atom as well as on the ring. For example, $\Delta G^{\ddagger}$ = 12.2 kcal mol^{-1} for rotation around the arene–metal bond in (1,4-*t*-$Bu_2C_6H_4$)Ru(CO)($SiCl_3$)$_2$: Pomeroy, R. K.; Harrison, D. J. *J. Chem. Soc., Chem. Commun.* **1980**, 661. The introduction of heteroatoms in the ring has a similar effect, though the origin is now electronic in nature. The barrier to internal rotation in tricarbonyl(borazine)chromium(0) is predicted[44a] to be ≥18.3 kcal mol^{-1}. In the case of **2** and **3**, neither steric nor electronic requirements for a high rotation barrier are met.

Table VI. Crystallographic Data for 1–4

	1	2	3	4
formula	$C_{18}H_{30}$	$C_{21}H_{30}CrO_3$	$C_{21}H_{30}MoO_3$	$C_{38}H_{45}CrO_2P$
space group	$P\bar{1}$	$P2_1/n$	$P2_1/n$	$P\bar{1}$
a (Å)	6.013 (5)	14.156 (6)	14.183 (3)	8.911 (3)
b (Å)	8.405 (5)	16.734 (4)	16.950 (8)	9.489 (3)
c (Å)	9.286 (3)	9.103 (3)	9.129 (2)	21.665 (7)
α (deg)	109.14 (3)			81.06 (2)
β (deg)	107.99 (5)	106.21 (2)	103.90 (2)	80.33 (2)
γ (deg)	95.59 (6)			65.89 (2)
Z	1	4	4	2
D_{calcd} (g cm^{-3})	0.994	1.226	1.329	1.248
μ(Cu Kα) (cm^{-1})	4.1	48.9	53.8	37.0
reflctns measd	1107	2795	2863	4415
reflctns obsd[a]	948	2417	2610	3877
R (R_w)	0.050 (0.062)	0.045 (0.051)	0.030 (0.038)	0.052 (0.061)
cryst size (mm)	0.15 × 0.15 × 0.50	0.30 × 0.35 × 0.40	0.25 × 0.25 × 0.35	0.10 × 0.20 × 0.40
max θ (deg)	57	57	57	57
least-squares refinement	full matrix	full matrix	full matrix	full matrix
absorptn correctn	no	yes	yes	yes
structure obtained	by multiple-solution procedure[b]	from 3	by heavy-atom method	by heavy-atom method
Hilger-Watts diffractometer (Ni-filtered Cu Kα radiation, θ-2θ scans, pulse-height discrimination)				

[a] Reflections were regarded as significant if $I > 2.5\sigma(I)$. [b] Germain, G.; Main, P.; Woolfson, M. M. *Acta Crystallogr., Sect. A* 1971, *A27*, 368.

analysis.[11] The crystals are triclinic, space group $P\bar{1}$. A stereoview of the X-ray structure is shown in Figure 8, deviations of the nonhydrogen atoms from the least-squares plane of the benzene ring are given in Figure 9,[46] and selected bond lengths, bond angles, and dihedral angles are reported in Tables I–III.

Upon comparison of Figures 8 and 9 with Figures 4 and 5, it becomes immediately apparent that replacement of a carbonyl group by triphenylphosphine leads to a striking change in the conformation of the arene moiety: whereas the conformations of **2** and **3** are eclipsed, with methyl groups alternately proximal and distal, in **4** the conformation is staggered and all six methyl groups are distal.[47] There are indications that the arene ligand in **4** adopts the observed conformation in reponse to the steric requirements of the triphenylphosphine group. Thus, the out-of-plane deviations of the methylene and methyl carbons C(24) and C(34) in **4** (−0.139 and −1.579 Å, respectively) are significantly larger than any corresponding deviations in **2** (Figure 5), evidently as a result of steric interference from one of the triphenylphosphine rings, C(51)–C(56) (Figure 8).[46] Furthermore, the Cr atom in **4** is offset slightly toward C(11) and C(12); the angle between the normal to the least-squares plane of the ring and the vector from X to the Cr atom is 2.5°, as compared to essentially zero in **2**. In consequence, the C(1)–Cr–C(2) plane in **4** is tilted toward C(11)–C(12). The concomitant shortening of the carbonyl distances from the least-squares plane is seen by comparison of carbonyl carbon and oxygen deviations in **2** (Figure 5) with those in **4** (Figure 9). These structural features lead to an increase in nonbonded interactions between the arene and $Cr(CO)_2PPh_3$ moieties, with the result that all the methyl groups are forced to the distal side and the arene assumes an insectile appearance.[48] With all the methyls distal, the view from the proximal side is now essentially the same as it would be in the corresponding hexamethylbenzene complex, and it is therefore not surprising that the molecule adopts the observed S(6) conformation.

Table VII. Final Atomic Parameters for **1**[a]

atom	x	y	z	B, Å^2
C(1)	0.3309 (3)	0.3481 (2)	0.4541 (2)	*b*
C(2)	0.3464 (3)	0.4145 (2)	0.3364 (2)	*b*
C(3)	0.5167 (3)	0.5658 (2)	0.3823 (2)	*b*
C(4)	0.1436 (4)	0.1861 (3)	0.4051 (3)	*b*
C(5)	0.1833 (4)	0.3206 (3)	0.1592 (3)	*b*
C(6)	0.5295 (4)	0.6402 (3)	0.2557 (2)	*b*
C(7)	−0.0942 (4)	0.2253 (3)	0.4150 (3)	*b*
C(8)	0.2904 (5)	0.1879 (3)	0.0611 (3)	*b*
C(9)	0.3660 (5)	0.7663 (3)	0.2401 (3)	*b*
H(4)A	0.208	0.120	0.478	4.0
H(4)B	0.116	0.108	0.289	4.0
H(5)A	0.147	0.408	0.107	4.0
H(5)B	0.026	0.259	0.155	4.0
H(6)A	0.485	0.540	0.146	4.0
H(6)B	0.700	0.701	0.286	4.0
H(7)A	−0.216	0.117	0.384	6.0
H(7)B	−0.161	0.289	0.344	6.0
H(7)C	−0.069	0.302	0.533	6.0
H(8)A	0.179	0.130	−0.054	6.0
H(8)B	0.326	0.101	0.112	6.0
H(8)C	0.446	0.250	0.064	6.0
H(9)A	0.372	0.810	0.154	6.0
H(9)B	0.408	0.862	0.347	6.0
H(9)C	0.192	0.701	0.207	6.0

[a] Standard deviations in parentheses. [b] Anisotropic thermal parameters are recorded in the Supplementary Material.

The disparity between the arene conformations in **2** and **4** persists in solution, as shown by a comparison of the 25.2-MHz $^{13}C\{^1H\}$ NMR spectra of the two complexes in CD_2Cl_2. In contrast to the behavior of **2**, no resonance doubling of the CH_3, CH_2, and C_{ar} carbon signals (Table V, Experimental Section) was observed down to −84 °C.[37,49] Furthermore, the carbonyl carbon resonance was not observable at ambient temperature and could be detected only at low temperatures or by using samples enriched in ^{13}CO. Both of these observations are consistent with a ground-state conformation in which, on the timescale of rapid rotation about the arene–metal bond,[50] the arene moiety effectively exhibits local

(46) The projection in Figure 9 corresponds to the mirror image of the stereoview in Figure 8.

(47) In roughly one out of every three molecules, a maverick methyl (C33B) is found on the proximal side, as a disorder in the crystal.

(48) There are additional, if less dramatic, differences between the structures of 4 and 2. Thus, although the average C_{ar}–C_{ar} bond length in 4 (1.424 Å) is not significantly larger than that in **2** (1.421 Å), individual distances vary considerably, from 1.404 to 1.435 Å (Table I).[33] However, in other respects interatomic distances in 4 are quite normal. The distance of the Cr atom from the least-squares arene plane and the average Cr–C_{ar} distances of 1.729 and 2.241 Å in **4** are comparable to the corresponding values of 1.725 and 2.235 Å in **2**. The Cr–P and average C–P bond lengths of 2.320 and 1.844 Å in 4 are comparable to the corresponding values of 2.337 and 1.836 Å reported for dicarbonyl(methoxycarbonylbenzene)(triphenylphosphine)chromium(0): Andrianov, V. G.; Struchkov, Y. T.; Baranetzkaya, N. K.; Setkina, V. N.; Kursanov, D. N. *J. Organomet. Chem.* **1975**, *101*, 209.

(49) At −125 °C in $CHFCl_2/C_6D_6$, the methyl and methylene resonances of 4 still appear as singlets; the aromatic resonance is obscured by solvent peaks. At 32 °C, changes in relative intensities and temperature-dependent chemical shifts are observed for these signals.

Table VIII. Final Atomic Parameters for 2[a]

atom	x	y	z	B, Å²
Cr	0.28417 (4)	0.14940 (3)	0.61868 (6)	b
O(1)	0.3215 (2)	0.3131 (2)	0.5188 (4)	b
O(2)	0.4999 (2)	0.1162 (2)	0.7255 (4)	b
O(3)	0.2937 (2)	0.2170 (2)	0.9257 (4)	b
C(1)	0.3088 (3)	0.2492 (2)	0.5595 (5)	b
C(2)	0.4160 (3)	0.1302 (2)	0.6852 (4)	b
C(3)	0.2904 (3)	0.1908 (2)	0.8070 (5)	b
C(11)	0.1217 (2)	0.1427 (2)	0.5066 (4)	b
C(12)	0.1727 (2)	0.1402 (2)	0.3923 (4)	b
C(13)	0.2457 (2)	0.0817 (2)	0.3976 (4)	b
C(14)	0.2703 (2)	0.0260 (2)	0.5207 (4)	b
C(15)	0.2211 (3)	0.0282 (2)	0.6369 (4)	b
C(16)	0.1473 (3)	0.0874 (2)	0.6292 (4)	b
C(21)	0.0384 (3)	0.2021 (2)	0.4948 (4)	b
C(22)	0.1469 (3)	0.1996 (2)	0.2613 (4)	b
C(23)	0.2953 (3)	0.0760 (2)	0.2693 (4)	b
C(24)	0.3456 (3)	−0.0383 (2)	0.5245 (4)	b
C(25)	0.2439 (3)	−0.0335 (2)	0.7644 (5)	b
C(26)	0.0937 (3)	0.0902 (2)	0.7530 (5)	b
C(31)	0.0681 (3)	0.2818 (2)	0.5741 (5)	b
C(32)	0.0664 (3)	0.1683 (3)	0.1252 (5)	b
C(33)	0.3902 (3)	0.1230 (3)	0.2924 (5)	b
C(34)	0.2991 (4)	−0.1131 (3)	0.4388 (6)	b
C(35)	0.3266 (4)	−0.0115 (3)	0.9056 (5)	b
C(36)	0.0012 (4)	0.0376 (3)	0.7118 (6)	b
H(21)A	−0.013	0.177	0.538	5.0
H(21)B	0.005	0.212	0.381	5.0
H(22)A	0.207	0.213	0.229	5.0
H(22)B	0.123	0.251	0.299	5.0
H(23)A	0.247	0.094	0.172	5.0
H(23)B	0.311	0.017	0.257	5.0
H(24)A	0.382	−0.052	0.631	6.0
H(24)B	0.396	−0.016	0.472	6.0
H(25)A	0.260	−0.086	0.722	6.0
H(25)B	0.182	−0.042	0.799	6.0
H(26)A	0.078	0.146	0.772	6.0
H(26)B	0.140	0.068	0.853	6.0
H(31)A	0.009	0.318	0.558	7.0
H(31)B	0.117	0.309	0.527	7.0
H(31)C	0.098	0.274	0.684	7.0
H(32)A	0.049	0.207	0.040	7.0
H(32)B	0.005	0.155	0.158	7.0
H(32)C	0.089	0.116	0.087	7.0
H(33)A	0.419	0.117	0.204	7.0
H(33)B	0.441	0.106	0.389	7.0
H(33)C	0.378	0.182	0.304	7.0
H(34)A	0.348	−0.155	0.438	8.0
H(34)B	0.263	−0.099	0.328	8.0
H(34)C	0.249	−0.135	0.487	8.0
H(35)A	0.339	−0.054	0.985	8.0
H(35)B	0.312	0.041	0.950	8.0
H(35)C	0.390	−0.003	0.874	8.0
H(36)A	−0.035	0.040	0.794	8.0
H(36)B	0.015	−0.019	0.694	8.0
H(36)C	−0.047	0.059	0.613	8.0

[a,b] See footnotes *a* and *b*, Table VII.

Table IX. Final Atomic Parameters for 3[a]

atom	x	y	z	B, Å²
Mo	0.29303 (2)	0.15085 (2)	0.62644 (3)	b
O(1)	0.3352 (3)	0.3183 (2)	0.5182 (5)	b
O(2)	0.5135 (2)	0.1139 (2)	0.7331 (4)	b
O(3)	0.2998 (3)	0.2180 (2)	0.9459 (4)	b
C(1)	0.3226 (3)	0.2556 (3)	0.5632 (5)	b
C(2)	0.4317 (3)	0.1299 (3)	0.6950 (5)	b
C(3)	0.2989 (3)	0.1939 (3)	0.8261 (5)	b
C(11)	0.1236 (2)	0.1408 (2)	0.5069 (4)	b
C(12)	0.1775 (2)	0.1380 (2)	0.3936 (4)	b
C(13)	0.2474 (3)	0.0775 (2)	0.3957 (4)	b
C(14)	0.2683 (3)	0.0229 (2)	0.5178 (4)	b
C(15)	0.2161 (3)	0.0251 (2)	0.6331 (4)	b
C(16)	0.1453 (3)	0.0858 (2)	0.6280 (4)	b
C(21)	0.0422 (3)	0.2013 (3)	0.4959 (4)	b
C(22)	0.1555 (3)	0.1966 (2)	0.2643 (4)	b
C(23)	0.2979 (3)	0.0701 (2)	0.2678 (4)	b
C(24)	0.3397 (3)	−0.0432 (2)	0.5173 (5)	b
C(25)	0.2341 (4)	−0.0365 (3)	0.7569 (5)	b
C(26)	0.0887 (3)	0.0890 (3)	0.7499 (5)	b
C(31)	0.0714 (3)	0.2792 (3)	0.5753 (6)	b
C(32)	0.0755 (3)	0.1674 (3)	0.1318 (5)	b
C(33)	0.3939 (3)	0.1143 (3)	0.2894 (6)	b
C(34)	0.2924 (4)	−0.1152 (3)	0.4321 (6)	b
C(35)	0.3144 (5)	−0.0169 (3)	0.8958 (5)	b
C(36)	−0.0031 (4)	0.0380 (3)	0.7095 (6)	b
H(21)A	0.013	0.213	0.384	5.0
H(21)B	−0.010	0.178	0.539	5.0
H(22)A	0.215	0.209	0.231	5.0
H(22)B	0.131	0.248	0.302	5.0
H(23)A	0.253	0.091	0.172	5.0
H(23)B	0.310	0.012	0.251	5.0
H(24)A	0.372	−0.058	0.625	6.0
H(24)B	0.392	−0.024	0.468	6.0
H(25)A	0.250	−0.088	0.715	6.0
H(25)B	0.172	−0.044	0.792	6.0
H(26)A	0.072	0.146	0.765	6.0
H(26)B	0.131	0.069	0.848	6.0
H(31)A	0.016	0.316	0.560	7.0
H(31)B	0.124	0.305	0.529	7.0
H(31)C	0.100	0.271	0.683	7.0
H(32)A	0.061	0.207	0.046	7.0
H(32)B	0.013	0.156	0.162	7.0
H(32)C	0.097	0.116	0.091	7.0
H(33)A	0.425	0.106	0.202	7.0
H(33)B	0.443	0.093	0.383	7.0
H(33)C	0.386	0.172	0.304	7.0
H(34)A	0.339	−0.159	0.434	8.0
H(34)B	0.259	−0.102	0.326	8.0
H(34)C	0.239	−0.136	0.483	8.0
H(35)A	0.325	−0.058	0.975	8.0
H(35)B	0.302	0.035	0.943	8.0
H(35)C	0.380	−0.009	0.865	8.0
H(36)A	−0.043	0.042	0.785	8.0
H(36)B	0.011	−0.017	0.691	8.0
H(36)C	−0.048	0.060	0.608	8.0

[a,b] See footnotes *a* and *b*, Table VII.

C_{6v} symmetry. Under these conditions, the six ethyl groups are symmetry equivalent, as are the six C_{ar} atoms, and are therefore isochronous. Furthermore, the increase in the average distance between the carbonyl carbons and the methyl hydrogens leads to an increase in spin-lattice relaxation time and to a loss of carbonyl carbon signal intensity. The conformational disparity between **2** and **4** is therefore not merely the result of crystal packing forces[52] but is the consequence of inherent molecular properties.

Experimental Section

Infrared spectra were recorded on a Perkin-Elmer 283 spectrometer. Solution 100.1-MHz ^1H and 25.2-MHz $^{13}C\{^1H\}$ NMR spectra were recorded on a Varian XL-100 spectrometer. Solution 89.55-MHz and 60-MHz ^1H NMR spectra were obtained on JEOL FX-90Q and Varian A60A spectrometers, respectively. Solid-state (neat) spectra were obtained on a JEOL FX-60QS spectrometer using cross polarization and magic angle spinning.[53] Mass spectra were measured on an AEI MS-9 high-resolution mass spectrometer with a DS-30 data system. An ionizing voltage of 70 eV was used. Photochemical reactions were performed in quartz vessels with a Hanovia high-pressure Hg UV source. Reagents obtained from the indicated sources were used without further purification: **1**, $Cr(CO)_6$ (Pfaltz & Bauer); $Mo(CO)_6$ (Strem); Ph_3P (Matheson Coleman & Bell); ^{13}CO (Stohler Isotope Co.). Tetrahydrofuran (THF)

(50) Dicarbonyl(1,3,5-tri-*tert*-butylbenzene)(triphenylphosphine)chromium(0), presumably a more sterically hindered system, shows no sign of slowed rotation about the arene–metal bond at −60 °C.[51]

(51) Jackson, W. R.; Pincombe, C. F.; Rae, I. D.; Rash, D.; Wilkinson, B. *Aust. J. Chem.* **1976**, *29*, 2431.

(52) The solid-state NMR spectrum of **4** (Table V, Experimental Section) features six aromatic and two carbonyl carbon signals. This site nonequivalence is due to the asymmetric location of the molecule in the crystal lattice. The observed equivalence of methyl and methylene carbons is due to accidental isochrony.[15]

(53) We thank Dr. Michael J. Albright of JEOL USA Inc. for these results.

Table X. Final Atomic Parameters for 4[a]

atom	x	y	z	B, Å²	atom	x	y	z	B, Å²
Cr	0.67611 (7)	0.67018 (7)	0.28382 (3)	b	H(23)A	0.764	0.256	0.292	7.0
P	0.63958 (12)	0.71732 (11)	0.17790 (5)	b	H(23)BB	0.836	0.238	0.372	7.0
O(1)	0.7142 (4)	0.9690 (3)	0.2796 (2)	b	H(23)BA	0.712	0.234	0.326	7.0
O(2)	1.0356 (4)	0.5095 (4)	0.2417 (2)	b	H(23)B	0.908	0.272	0.325	7.0
C(1)	0.7023 (5)	0.8504 (5)	0.2786 (2)	b	H(24)A	0.571	0.343	0.258	7.0
C(2)	0.8949 (5)	0.5732 (5)	0.2569 (2)	b	H(24)B	0.396	0.491	0.248	7.0
C(11)	0.6185 (5)	0.6933 (5)	0.3854 (2)	b	H(25)A	0.270	0.703	0.254	7.0
C(12)	0.7254 (5)	0.5352 (4)	0.3760 (2)	b	H(25)B	0.232	0.867	0.281	7.0
C(13)	0.6763 (5)	0.4499 (4)	0.3410 (2)	b	H(26)A	0.426	0.989	0.370	7.0
C(14)	0.5252 (5)	0.5189 (4)	0.3140 (2)	b	H(26)B	0.292	0.979	0.330	7.0
C(15)	0.4223 (5)	0.6781 (5)	0.3219 (2)	b	H(31)A	0.645	0.833	0.517	7.0
C(16)	0.4651 (5)	0.7629 (4)	0.3585 (2)	b	H(31)B	0.657	0.659	0.512	7.0
C(21)	0.6674 (6)	0.7830 (6)	0.4245 (2)	b	H(31)C	0.486	0.809	0.501	7.0
C(22)	0.8872 (6)	0.4587 (6)	0.4050 (2)	b	H(32)A	0.984	0.334	0.488	7.0
C(23)	0.7860 (6)	0.2809 (5)	0.3332 (3)	b	H(32)B	0.827	0.302	0.474	7.0
C(24)	0.4700 (6)	0.4220 (5)	0.2814 (2)	b	H(32)C	0.796	0.465	0.500	7.0
C(25)	0.2581 (5)	0.7521 (6)	0.2934 (2)	b	H(33)A	0.858	0.060	0.368	7.0
C(26)	0.3543 (6)	0.9311 (5)	0.3681 (2)	b	H(33)BC	0.878	0.250	0.248	7.0
C(31)	0.6092 (7)	0.7704 (6)	0.4941 (2)	b	H(33)BB	1.003	0.254	0.294	7.0
C(32)	0.8726 (6)	0.3847 (5)	0.4717 (2)	b	H(33)BA	0.956	0.103	0.300	7.0
C(33)	0.7791 (8)	0.1634 (7)	0.3795 (3)	b	H(33)B	0.664	0.169	0.387	7.0
C(33)B	0.9125 (22)	0.2181 (19)	0.2901 (8)	7.0	H(33)C	0.808	0.186	0.420	7.0
C(34)	0.3782 (5)	0.3350 (5)	0.3259 (2)	b	H(34)A	0.343	0.272	0.302	7.0
C(35)	0.1142 (5)	0.7347 (5)	0.3374 (3)	b	H(34)B	0.275	0.412	0.348	7.0
C(36)	0.2298 (6)	0.9576 (5)	0.4253 (2)	b	H(34)C	0.450	0.264	0.358	7.0
C(41)	0.8147 (5)	0.7401 (4)	0.1236 (2)	b	H(35)A	0.008	0.786	0.318	7.0
C(42)	0.8754 (6)	0.8443 (6)	0.1348 (2)	b	H(35)B	0.098	0.787	0.377	7.0
C(43)	1.0065 (6)	0.8663 (6)	0.0961 (3)	b	H(35)C	0.136	0.623	0.350	7.0
C(44)	1.0781 (6)	0.7842 (5)	0.0455 (2)	b	H(36)A	0.162	1.070	0.428	7.0
C(45)	1.0199 (6)	0.6816 (6)	0.0330 (2)	b	H(36)B	0.289	0.913	0.464	7.0
C(46)	0.8882 (6)	0.6596 (5)	0.0713 (2)	b	H(36)C	0.154	0.903	0.424	7.0
C(51)	0.6158 (5)	0.5618 (4)	0.1454 (2)	b	H(42)	0.822	0.907	0.173	6.0
C(52)	0.7464 (5)	0.4159 (5)	0.1479 (2)	b	H(43)	1.048	0.944	0.106	7.0
C(53)	0.7338 (7)	0.2885 (5)	0.1299 (2)	b	H(44)	1.173	0.800	0.017	7.0
C(54)	0.5904 (8)	0.3029 (6)	0.1090 (3)	b	H(45)	1.074	0.618	−0.005	6.0
C(55)	0.4591 (7)	0.4452 (7)	0.1074 (3)	b	H(46)	0.844	0.583	0.061	5.0
C(56)	0.4711 (6)	0.5735 (5)	0.1252 (2)	b	H(52)	0.853	0.403	0.166	5.0
C(61)	0.4736 (5)	0.8955 (4)	0.1482 (2)	b	H(53)	0.831	0.183	0.130	6.0
C(62)	0.4376 (5)	0.9214 (5)	0.0862 (2)	b	H(54)	0.578	0.210	0.095	7.0
C(63)	0.3156 (6)	1.0589 (6)	0.0653 (2)	b	H(55)	0.350	0.455	0.094	7.0
C(64)	0.2295 (6)	1.1734 (6)	0.1052 (3)	b	H(56)	0.372	0.679	0.125	6.0
C(65)	0.2649 (6)	1.1510 (5)	0.1660 (3)	b	H(62)	0.504	0.837	0.056	5.0
C(66)	0.3864 (5)	1.0120 (5)	0.1879 (2)	b	H(63)	0.289	1.073	0.020	6.0
H(21)A	0.622	0.897	0.408	7.0	H(64)	0.138	1.274	0.090	6.0
H(21)B	0.793	0.747	0.419	7.0	H(65)	0.203	1.236	0.195	6.0
H(22)A	0.936	0.537	0.404	7.0	H(66)	0.413	0.993	0.233	5.0
H(22)B	0.967	0.374	0.377	7.0					

[a,b] See footnotes *a* and *b*, Table VII.

was distilled from $LiAlH_4$. All reactions were carried out under a nitrogen atmosphere.

Tricarbonyl(hexaethylbenzene)chromium(0) (2) was prepared by refluxing **1** (0.60 g, 2.43 mmol) and $Cr(CO)_6$ (0.55 g, 2.5 mmol) in a heptane (30 mL)/THF (5 mL) solution for 1 week.[54] The solvents were stripped off under reduced pressure, and the unreacted starting materials were removed by sublimation (85 °C[55] (0.5 torr)). The residue was triturated (under nitrogen) with CH_2Cl_2 and filtered. After removal of solvent, the filtrate yielded pale yellow crystals of **2** (0.19 g, 20%). Although **2** decomposes in solution, crystals of satisfactory quality were obtained by slow evaporation, under nitrogen, of CH_2Cl_2, CH_2Cl_2/heptane, or heptane solutions. Mass spectrum, *m/e* (relative intensity) 382 (M^+, 40), 326 ($M^+ - 2CO$, 37), 298 ($M^+ - 3CO$, 100); mass spectrum (high resolution), *m/e* 382.1603 (382.1599 calcd for $C_{21}H_{30}{}^{52}CrO_3$); IR (CCl_4) 1880, 1955 cm^{-1} (lit.[56a] ν(KBr) 1852, 1940 cm^{-1}; lit.[56] ν(cyclohexane) 1886, 1959 cm^{-1}). NMR properties are listed in Table V.

Tricarbonyl(hexaethylbenzene)molybdenum(0) (3) was similarly prepared from **1** (2.70 g, 11.0 mmol) and $Mo(CO)_6$ (3.21 g, 12.2 mmol) in refluxing heptane (30 mL). The reaction was continued for 1 week and after workup (as described above) yielded yellow crystals of **3** (2.85 g, 61%). Crystals of satisfactory quality could be grown from hot heptane or by slow evaporation, under nitrogen, of CH_2Cl_2/CCl_4 solutions. Mass spectrum, *m/e* (relative intensity) 428 (M^+, 32), 400 ($M^+ - CO$, 26), 372 ($M^+ - 2CO$, 29); mass spectrum (high resolution), *m/e* 428.1272 (428.1249 calcd for $C_{21}H_{30}{}^{98}MoO_3$); IR (CCl_4) 1875, 1955 cm^{-1}. NMR properties are listed in Table V.

Dicarbonyl(hexaethylbenzene)(triphenylphosphine)chromium(0) (4) crystallized from a freeze–thaw degassed heptane (30 mL) solution of **2** (0.22 g, 0.57 mmol) and Ph_3P (0.45 g, 1.7 mmol) upon UV irradiation (1.5 h). The orange-yellow product (0.19 g, 54%) was collected by filtration under a nitrogen atmosphere. The product could be recrystallized from benzene/heptane or benzene/cyclohexane solutions. Mass spectrum, *m/e* (relative intensity) 616 (M^+, 17), 560 ($M^+ - 2CO$, 100); mass spectrum (high resolution), *m/e* 616.2511 (616.2562 calcd for $C_{38}H_{45}{}^{52}CrO_2P$); IR (KBr) 1804, 1859 cm^{-1}.[57] NMR properties are listed in Table V.

^{13}CO-Labeling Experiments. Following the method of Strohmeier and von Hobe,[59] a solution of **2** (0.33 g, 0.88 mmol) in heptane (55 mL) was frozen in a liquid-nitrogen bath, and the reaction vessel was evacuated. After the reaction mixture was thawed, ^{13}CO (90% isotopically pure) was bled into the system. The pressure of the ^{13}CO was adjusted to 1 atm, and the magnetically stirred reaction mixture was irradiated with UV

(54) Without added THF, the reaction between $Cr(CO)_6$ and **1** proceeds only to a negligible extent.

(55) Substantial decomposition occurs at higher temperatures.

(56) (a) Fischer, R. D. *Chem. Ber.* **1960**, *93*, 165. (b) Fischer, R. D. *Spectrochim. Acta* **1963**, *19*, 842.

(57) The carbonyl stretching frequencies for **4** (relative to **2**) are consistent with earlier studies.[51,58]

(58) Howell, B. A.; Trahanovsky, W. S. *J. Am. Chem. Soc.* **1975**, *97*, 2136.

(59) Strohmeier, W.; von Hobe, D. *Z. Naturforsch., B: Anorg. Chem. Org. Chem.*, **1963**, *18B*, 770.

light for 2 h. Little decomposition was observed. The product was recovered by removing the heptane under reduced pressure. Of the total carbonyl content, 49% was ^{13}CO, as determined by mass spectroscopy. The relative amounts of $(C_6Et_6)Cr(^{13}CO)_3$ (11.9%), $(C_6Et_6)Cr(^{13}CO)_2(CO)$ (36.8%), $(C_6Et_6)Cr(^{13}CO)(CO)_2$ (38.1%), and $(C_6Et_6)Cr(CO)_3$ (13.2%) were calculated on the basis of stepwise equilibria.[60] The distribution of mass spectral peak intensities calculated for this statistical mixture matched the experimental data.

Variable-Temperature NMR Measurements. All variable-temperature $^{13}C\{^1H\}$ NMR spectra were recorded at 25.2 MHz in the Fourier transform mode on a Varian XL-100 spectrometer. All NMR samples were freeze–thaw degassed and sealed in 10-mm od sample tubes. Temperatures were measured with a copper-constantan thermocouple which was inserted, at coil height, into another 10-mm od sample tube containing an equal volume of the NMR solvent. Temperatures are considered to be accurate to ± 2 °C. Rates of exchange were measured in the temperature ranges of 223–273 K and 205–255 K for **2** and **3**, respectively.[62] The spin–lattice relaxation times (T_1) were obtained by the standard $(180°-\tau-90°-AT-PD)_n$ pulse sequence.[43b] Each T_1 determination was made from a linear least-squares fit of ten τ values. Pulse delays of $>5T_1$ were used.[63] The gated-decoupling technique[64] was used to determine the NOE's. Pulse delays of $\geq 10T_1$ were used in these experiments.[65] Sweep widths of 500 Hz and 8K Fourier transforms were used to ensure adequate digitization. Material labeled with ^{13}CO was used to substantially improve the signal/noise ratio obtained from the accumulation of two to ten transients.

Crystallography. Crystals suitable for X-ray analysis were obtained by slow crystallization from acetone (**1**), heptane (**2**, **3**), and heptane/benzene (**4**). The crystallographic data and details of data collection are reported in Table VI. Final atomic parameters for **1–4** are listed in Tables VII–X, respectively. The final difference map had no peaks greater than ±0.2, ±0.8, ±0.6, and ±0.6 eÅ^{-3} for **1–4**, respectively.

Acknowledgment. We thank the National Science Foundation (Grant CHE-8009670) for support of this work.

Supplementary Material Available: Final anisotropic thermal parameters with standard deviations for **1–4** (Tables XI–XIV) (4 pages). Ordering information is given on any current masthead page.

(60) The ratios of the stepwise formation constants used in these calculations were based on statistical arguments.[61] An isotope effect of unity was assumed for the exchange of free and complexed CO.

(61) Cotton, F. A.; Wilkinson, G. "Advanced Inorganic Chemistry", 3rd ed.; Interscience: New York, 1972; p 649.

(62) Experimental rate constants, in s^{-1} (temp, K), are 18 (223), 42 (232), 76 (237), 230 (246), 2150 (269), and 2750 (273) for **2** and are 2 (205), 40 (231), 77 (234), 185 (244), 350 (250), 600 (254), and 643 (256) for **3**.

(63) Harris, R. K.; Newman, R. H. *J. Magn. Reson.* **1976**, *24*, 449.

(64) Freeman, R.; Hill, H. D. W.; Kaptein, R. *J. Magn. Reson.* **1972**, *7*, 327.

(65) Canet, D. *J. Magn. Reson.* **1976**, *23*, 361.

Single-Crystal Polarized X-ray Absorption Spectroscopy. Observation and Theory for $(MoO_2S_2)^{2-}$

Frank W. Kutzler,† R. A. Scott,† Jeremy M. Berg,† Keith O. Hodgson,*† S. Doniach,‡ S. P. Cramer,§ and C. H. Chang§

Contribution from the Department of Chemistry and the Department of Applied Physics, Stanford University, Stanford, California 94305, and Exxon Research and Engineering Company, Linden, New Jersey 07036. *Received January 7, 1981*

Abstract: Linearly polarized synchrotron radiation has been used to investigate the orientation dependence of the K absorption edge of a single crystal of ammonium dithiomolybdate, the crystal structure of which is also reported herein. Following the collection of spectra with the polarization vector parallel to the oxygen–oxygen interatomic vector, the sulfur–sulfur vector, and the twofold rotation axis, self-consistent field Xα multiple scattered wave (SCF Xα MSW) calculations were done to interpret the observed orientation dependence. It is shown that this orientation dependence can be used to highlight the edge features which derive from molecular orbitals contributed to principally by the oxygen or the sulfur ligands. Anisotropy is also apparent in the extended X-ray absorption fine structure (EXAFS) spectra, which were recorded for orientations along the S–S and O–O interatomic vectors. It is thus demonstrated that polarized single-crystal X-ray absorption spectroscopy can provide orientationally selective information about the absorbing atom. It could, in principle, be used to deduce certain types of geometric information about the X-ray absorbing species.

Structural determination by X-ray diffraction requires long-range order in the sample. One of the primary advantages of the extended X-ray absorption fine structure (EXAFS) technique is that the absorbing atom need not be oriented in an extended array or lattice. Most of the X-ray absorption studies done heretofore have taken advantage of this freedom, measuring spectra for randomly oriented samples in solution, as powder, or as amorphous materials. The synchrotron radiation emitted from an electron storage ring is, however, linearly polarized in the horizontal plane and is well suited for use in absorption studies of oriented single crystals. The combination of oriented sample and polarized beam permits determination of the angular dependence of the absorption spectrum. The polarization effects can thus provide angularly selected structural information since the X-ray absorption spectrum contains information about the distances to, numbers of, and types of atoms surrounding the absorber.

In this paper we demonstrate the use of these effects in a study of the orientational dependence of the Mo K-edge absorption spectrum of ammonium dithiomolybdate, $(NH_4)_2MoO_2S_2$. The case of dithiomolybdate chosen for this study is particularly illustrative because the spectra from different orientations can be compared with those of molybdate and thiomolybdate which have been previously studied in experimental and theoretical detail.[1] In addition, the shape of the edges for different angles between the dithiomolybdate molecule and the polarization vector is interpreted by using molecular orbitals calculated from the self-consistent field Xα multiple scattered wave (SCF Xα MSW) formalism, which we have described earlier.[1] Also, we report here

† Department of Chemistry, Stanford University.
‡ Department of Applied Physics, Stanford University.
§ Exxon Research and Engineering Company.

(1) Kutzler, F. W.; Natoli, C. R.; Misemer, D. K.; Doniach, S.; Hodgson, K. O. *J. Chem. Phys.* **1980**, *73*, 3274.

0002-7863/81/1503-6083$01.25/0